Science Advances
AAAS

Supplementary Materials for

Origin of sulfur allotropes on the carbonaceous asteroid Ryugu and implications to the sulfur chemistry in the interstellar medium

Mason McAnally *et al.*

Corresponding author: Ralf I. Kaiser, ralfk@hawaii.edu

Sci. Adv. **12**, eaeb3358 (2026)
DOI: 10.1126/sciadv.aeb3358

This PDF file includes:

Quantification of S_8 by reflectron time-of-flight mass spectrometry

To quantify the amount of octasulfur produced in each ice, the reflectron time-of-flight mass spectrometer (ReToF-MS) was calibrated by using an experiment that ionizes both H_2S and S_8 at 10.49 eV.(*41*)

First, the molecules of H_2S (N_{H_2S}) were calculated in the infrared spectrum before irradiation utilizing the Fourier transform infrared (FTIR) spectrometer and the corresponding band strength of H_2S (Equation (1); Supplementary Table 8).

$$N_{H_2S} = \frac{\ln(10) \int_{\bar{\nu}_1}^{\bar{\nu}_2} A(\bar{\nu}) d\bar{\nu} \cos(\beta)}{2 A_{exp}} \quad (1)$$

Where, $\int_{\bar{\nu}_1}^{\bar{\nu}_2} A(\bar{\nu}) d\bar{\nu}$ is the integrated peak area in wavenumbers, A_{exp} is the band strength of the corresponding vibrational mode, and β is the angle at which the refracted light passes through the ice relative to surface normal calculated through Snell's Law (Equation (2)).

$$\beta = \sin^{-1} \frac{n_v}{n_{ice}} \sin(\theta) \quad (2)$$

Snell's law relates the angle of incidence of the infrared beam ($\theta = 43°$) to surface normal based on the ratio of refractive index between vacuum ($n_v = 1$) and the refractive index of the corresponding ice (n_{ice}; Supplementary Table 1).

Since the total number of H_2S molecules is known we can relate this to the integrated counts of the H_2S in the mass spectrum ($\int_{T_1}^{T_2} \chi_{H_2S} dT$) during temperature programmed desorption. This integration of the counts in the mass spectra (χ) over the desorbing temperatures (T_1 and T_2) provides the total signal from the ReToF-MS. The relation (τ) between the integrated counts detected by the ReToF-MS and FTIR provides a conversion factor between the two instruments (Equation (3)).

$$\tau = \frac{N_{H_2S}}{\int_{T_1}^{T_2} \chi_{H_2S} dT} \quad (3)$$

Since the photoionization cross section of each molecule is dependent on the wavelength of vacuum ultraviolet light, Equation (3) must be corrected for differences in these cross sections by applying a ratio (ξ) of photoionization cross sections of H_2S at 10.49 eV (σ_1) and S_8 at 9.34 eV (σ_2) (Equation (4)).

$$\xi = \frac{\sigma_1}{\sigma_2} \tag{4}$$

Combining Equation 3 and 4 with the integrated counts of S_8 ($\int_{T_1}^{T_2} \chi_{S_8} dT$) in the mass spectrum of each ice experiment provides the total S_8 produced within the ice (Equation (5)).

$$N_{S_8} = \tau\xi \int_{T_1}^{T_2} \chi_{S_8} dT \tag{5}$$

With the amount of octasulfur (S_8) produced upon electron irradiation known, further calculations were performed to determine the percent yield and conversion yield for each experiment. A correction for electron penetration depth (δ), calculated using CASINO v2.42, was applied to estimate the fraction of sulfur-bearing reagents (H_2S and SO_2) exposed to energetic electrons. This correction relates the total ice thickness (d_{ice}) to the maximum electron penetration depth (d_e) (Equation (6); Supplementary Tables 1 and 9).

$$\delta = \frac{d_e}{d_{ice}} \tag{6}$$

Combining Equations (1), (2), and (6) gives the total number of reactants (N_{rct}) exposed to energetic electrons (Equation (7)).

$$N_{rct} = \frac{\ln(10) \int_{\bar{\nu}_1}^{\bar{\nu}_2} A(\bar{\nu}) d\bar{\nu} \ \cos\left(\sin^{-1}\frac{n_v}{n_{ice}}\sin(\theta)\right)\delta}{2\, A_{exp}} \tag{7}$$

This calculation was performed for each sulfur-bearing component in the ice, and the results were summed to determine the total number of sulfur atoms exposed to energetic electrons. By comparing the total sulfur atoms in this region with the number of sulfur atoms converted to S_8, we calculate the percent yield of S_8 produced after irradiation (Equation (8)).

$$Percent\ Yield = \frac{8N_{S_8}}{N_{rct}} \cdot 100 \tag{8}$$

Conversion yields (in molecules eV^{-1}) were determined by calculating the total energy deposited into the ice by 5 keV electrons over the course of the 1-hour irradiation at 100 nA. To account for electron backscattering, dose corrections were applied using simulations from CASINO v2.42. The total energy deposited during the experiment was $1.1 \pm 0.2 \times 10^{19}$ eV. The conversion yield was then obtained by dividing the total number of octasulfur (S_8) molecules produced by the deposited dose (Equation (9)).

$$Conversion\ Yield = \frac{N_{S_8}}{Dose} \tag{9}$$

Table S1. Experimental parameters for the sulfur-bearing ices.

Experiment	Ice Composition	Irradiation Current (nA)	Irradiation Time (min)	Energy (eV)	Ice Ratio*	Ice Thickness (nm)	Refractive Index (n)
1	H_2S/H_2O	100	60	9.34	1 : 1.3	1150 ± 60	1.34
2	SO_2	100	60	9.34	-	1150 ± 60	1.33
3	SO_2/H_2O	100	60	9.34	1 : 1.4	1120 ± 60	1.30
4	SO_2/H_2S	100	60	9.34	1.3 : 1	1090 ± 100	1.37
5	H_2S/H_2O	100	60	8.75	1 : 1.2	1090 ± 50	1.34
6	SO_2	100	60	8.75	-	1180 ± 60	1.33
7	SO_2/H_2O	100	60	8.75	1 : 1.4	1180 ± 60	1.30
8	SO_2/H_2S	100	60	8.75	1.2 : 1	950 ± 90	1.37

*Error in ice ratio calculations is ± 0.2

Table S2. Infrared absorption assignments for the SO_2 ice experiment.

Peak Position (cm^{-1})	Assignment	Reference
Before Irradiation		
2461	$\nu_1 + \nu_3$ SO_2	(*70*)
2290	$2\nu_1$ SO_2	(*70*)
1325	ν_3 SO_2	(*70*)
1314	ν_3 SO_2	(*70*)
1147	ν_1 SO_2	(*70*)
After Irradiation		
2457	$\nu_1 + \nu_3$ SO_2	(*70*)
2288	$2\nu_1$ SO_2	(*70*)
1401	ν_3 SO_3	(*35*)
1388	ν_3 SO_3	(*35*)
1343, 1319, 1310	ν_3 SO_2	(*35*)
1146	ν_1 SO_2	(*70*)

Table S3. Infrared absorption assignments for the SO_2/H_2O experiments.

Peak Position (cm^{-1})	Assignment	Reference
Before Irradiation		
3599, 3368, 3222, 3184, 3114	ν_1/ν_3 H_2O	(*33*)
2466	$\nu_1 + \nu_3$ SO_2	(*70*)
2185	?	
1655, 1540	ν_2 H_2O	(*33*)
1325	ν_3 SO_2	(*70*)
1152	ν_1 SO_2	(*70*)
811	ν_L H_2O	(*33*)
After Irradiation		
3603	ν_1/ν_3 H_2O	(*33*)
3566	ν(OH)	(*38*)
3496	ν(OH)	(*38*)
3409, 3252	ν_1/ν_3 H_2O	(*33*)
3110, 2983, 2468, 2466, 2141	ν(OH)	(*38*)
1833	δ(HOH)	(*38*)
1708, 1645, 1562	ν_2 H_2O	(*33*)
1338, 1331, 1322, 1311	ν_3 SO_2	(*70*)
1288	ν(S=O)	(*38*)
1226	ν(S=O)	(*38*)
1151, 1142	ν_1 SO_2	(*70*)
1137	δ(SOH)	(*38*)
1089	ν(S=O)	(*38*)
1049	ν(S–O)	(*38*)
1023	ν(S–O)	(*38*)
975	ν(S–OH)	(*38*)
898	ν(S–OH)	(*38*)
852, 774	ν_L H_2O	(*33*)

Note. “L” defines the lattice vibration

Table S4. Infrared absorption assignments for the SO_2/H_2S experiments.

Peak Position (cm^{-1})	Assignment	Reference
Before Irradiation		
2596	ν_3 H_2S	(*34*)
2557	ν_1 H_2S	(*34*)
2456	$\nu_1 + \nu_3$ SO_2	(*70*)
2286	$2\nu_1$ SO_2	(*70*)
2042	ν_3 OCS	(*35*)
1319	ν_3 SO_2	(*70*)
1171	ν_2 H_2S	(*34*)
1145	ν_1 SO_2	(*70*)
After Irradiation		
3573, 3404, 3251, 3002, 2682	ν(OH)	(*38*)
2589	ν_3 H_2S	(*34*)
2554	ν_1 H_2S	(*34*)
2488	ν(SH) H_2S_x	(*36*, *37*)
2453	$\nu_1 + \nu_3$ SO_2	(*70*)
2391	ν(OH) acid	(*38*)
2362	ν(OH) acid	(*38*)
2339	ν(OH) acid	(*38*)
2311	ν(OH) acid	(*38*)
2284	ν(OH) acid	(*38*)
2039	ν(OH) acid	(*38*)
1718	δ(HOH) H_3O^+	(*38*)
1327, 1314, 1311	ν_3 SO_2	(*70*)
1298, 1268, 1214, 1184	ν(S=O)	(*38*)
1167	ν_2 H_2S	(*34*)
1145	ν_1 SO_2	(*70*)
1130	δ(SOH)	(*38*)
1120, 1083	ν(S=O)	(*38*)
806	ν(S–OH)	(*38*)

Table S5. Infrared absorption assignments for the H_2S/H_2O experiments.

Peak Position (cm^{-1})	Assignment	Reference
Before Irradiation		
3510, 3391, 3292, 3188, 2963	ν_1/ν_3 H_2O	(*33*)
2544	ν_3 H_2S	(*34*)
2505	ν_3 H_2S	(*34*)
2038	ν_3 OCS	(*71*)
1635	ν_2 H_2O	(*33*)
1171	ν_2 H_2S	(*34*)
830, 742	ν_L H_2O	(*33*)
After Irradiation		
3489, 3408, 3318, 3170	ν_1/ν_3 H_2O	(*33*)
2931, 2693	ν(OH)	(*38*)
2544, 2505	ν_3 H_2S	(*34*)
2477	ν(SH) H_2S_x	(*36*, *37*)
2038	ν_3 OCS	(*35*)
1635	ν_2 H_2O	(*33*)
1171	ν_2 H_2S	(*34*)
830, 742	ν_L H_2O	(*33*)

Note. “L” defines the lattice vibration

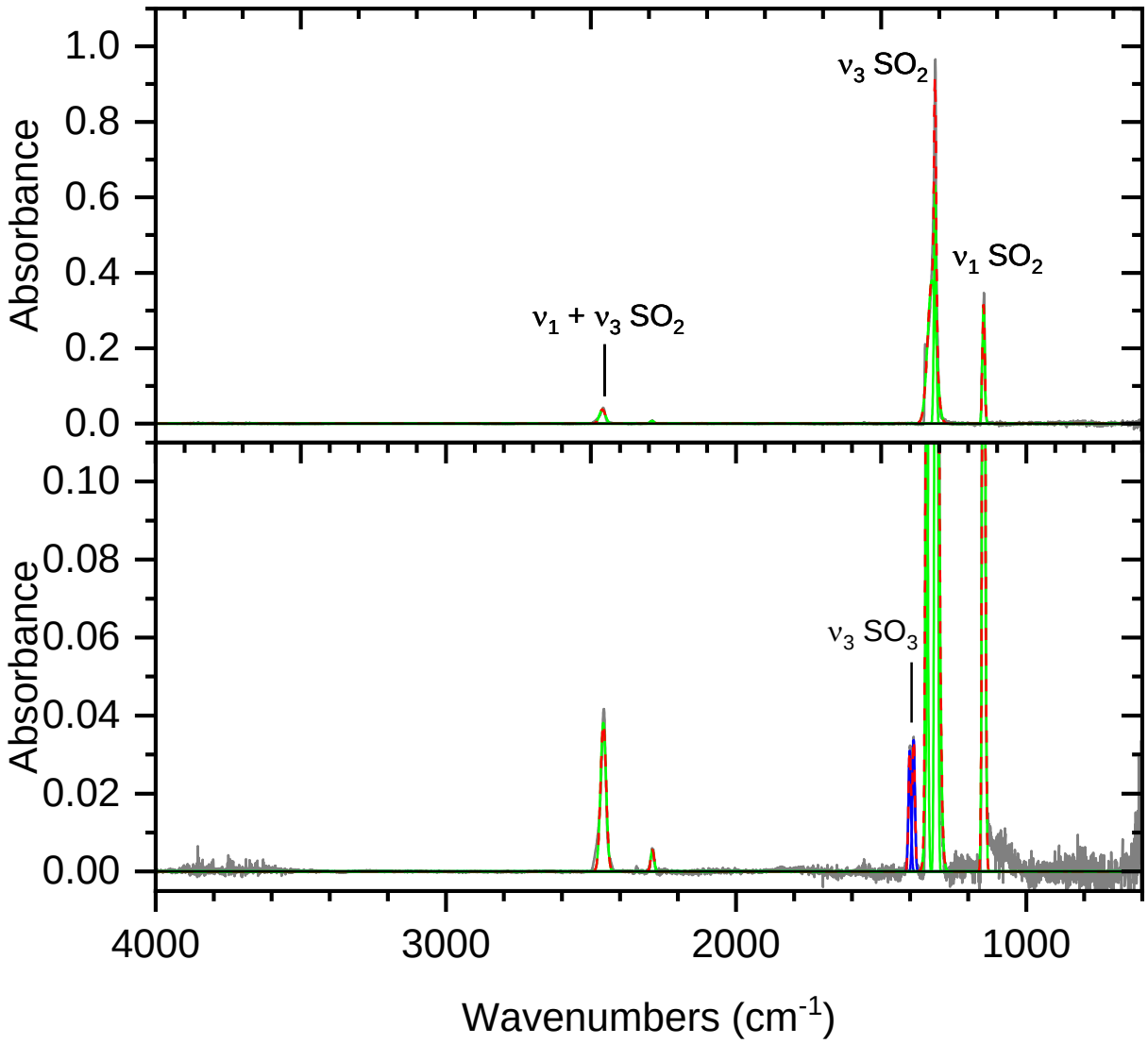

Figure S1. FTIR spectra of sulfur dioxide (SO_2) ice before (top) and after (bottom) irradiation. The spectra are deconvoluted to reveal functional groups related to the reagents (green) and products (blue).

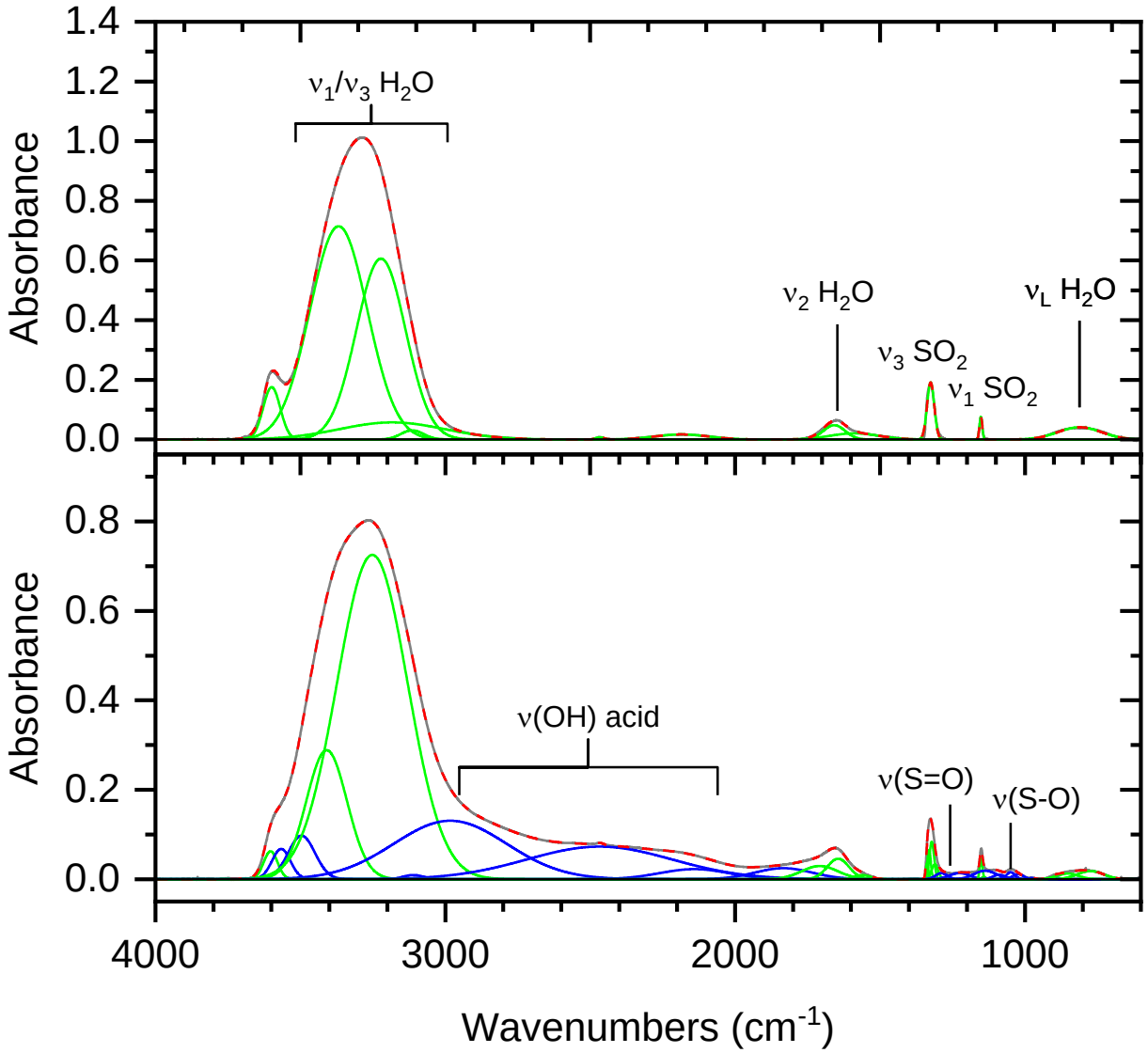

Figure S2. FTIR spectra of sulfur dioxide (SO_2)/water (H_2O) ice before (top) and after (bottom) irradiation. The spectra are deconvoluted to reveal functional groups related to the reagents (green) and products (blue).

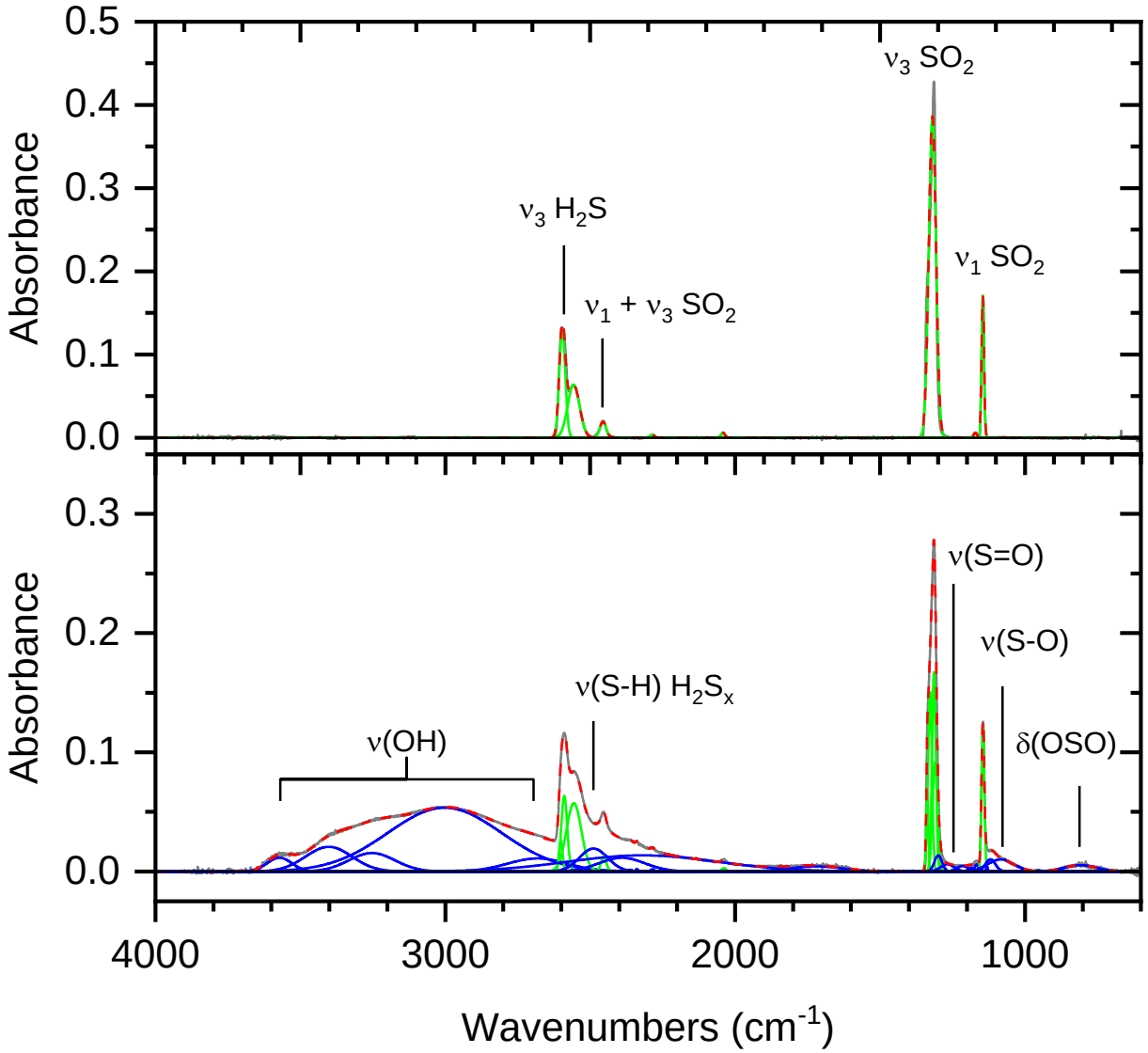

Figure S3. FTIR spectra of sulfur dioxide (SO_2)/hydrogen sulfide (H_2S) ice before (top) and after (bottom) irradiation. The spectra are deconvoluted to reveal functional groups related to the reagents (green) and products (blue). Sulfanes (H_2S_x; where $x \geq 2$) overlap and cannot be deconvoluted from one another.

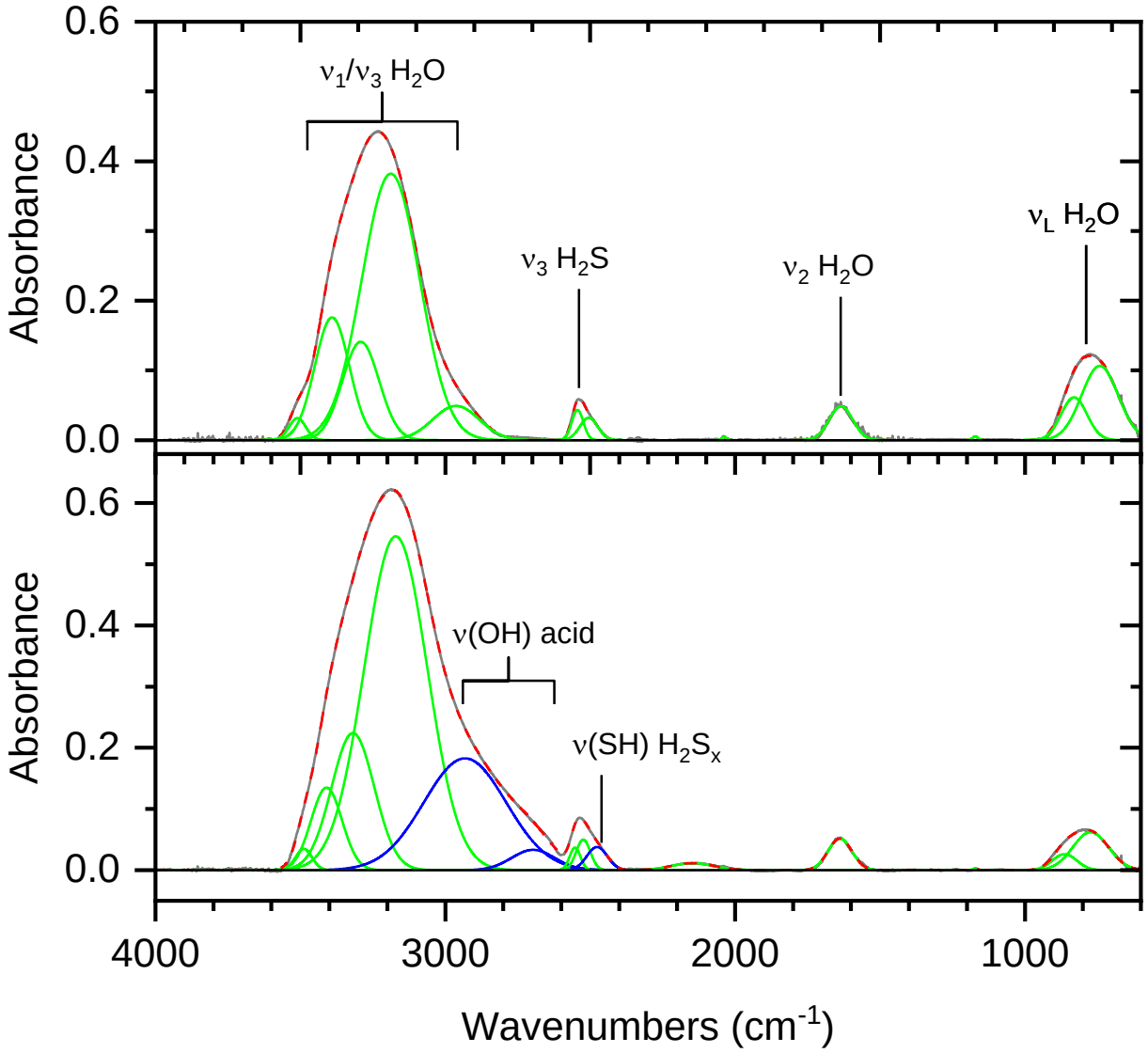

Figure S4. FTIR spectra of hydrogen sulfide (H_2S)/water (H_2O) ice before (top) and after (bottom) irradiation. The spectra are deconvoluted to reveal functional groups related to the reagents (green) and products (blue). Sulfanes (H_2S_x; where $x \geq 2$) overlap and cannot be deconvoluted from one another.

Table S6: Error analysis of adiabatic ionization energies (IEs) and relative energies of distinct S_8 isomers **a-f** (*m/z* = 256); IEs and relative energies were calculated with F12-TZ//B3LYP/aug-cc-pVTZ and F12-TZ//B3LYP/aVTZ levels of theory including zero-point vibrational energy corrections. The IE ranges are corrected for the thermal and Stark effect by –0.03 eV and the combined error limits of –0.05/+0.05 eV.(*41*)

	S_8 isomer	**Structure**	**Relative energy (kJ mol^{-1})**	**IE (eV)**	**IE range with error (eV)**	**Corrected IE with Stark effect (eV)**
1	**a:** Crown	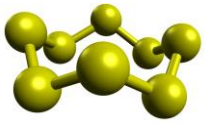	0	8.85 ± 0.05	8.80 – 8.90	8.77 – 8.87
2	**b:** Cluster chain	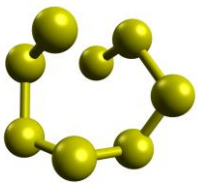	70	8.61 ± 0.05	8.56 – 8.66	8.53 – 8.63
3	**c:** S_7S	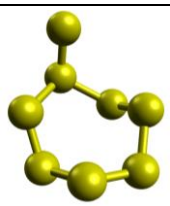	109	8.31 ± 0.05	8.26 – 8.36	8.23 – 8.33
4	**d:** Boat	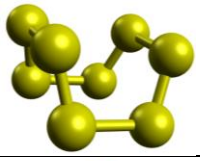	69	8.30 ± 0.05	8.25 – 8.35	8.22 – 8.32
5	**e:** C_{2h}	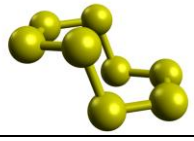	67	8.26 ± 0.05	8.21 – 8.31	8.18 – 8.28
6	**f:** Chair	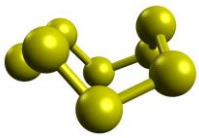	39	8.20 ± 0.05	8.15 – 8.25	8.12 – 8.22

Table S7. Parameters for the generation of VUV light utilizing difference four-wave mixing. The resulting photon energy has an uncertainty of less than 0.001 eV.

Experiment	Medium	ω_{VUV}	ω_1 (nm)	YAG 1 Wavelength (nm)	ω_1 Dye	YAG 2 Wavelength (nm)	ω_2 (nm)	Energy (eV)
1, 2, 3	Krypton	$2\omega_1 - \omega_2$	212.556	355	Stilbene 420	532	532[a]	9.34
4, 5, 6	Krypton	$2\omega_1 - \omega_2$	212.556	355	Stilbene 420	-	425.112	8.75

[a]Nd:YAG harmonic

Table S8. Physical parameters of each ice reagent used in these experiments.

Ice Component	Density (g cm^{-3})	Peak Position (cm^{-1})	Band Strength (cm $molecule^{-1}$)	Refractive Index (n)	Reference
H_2S	0.944(*62*)	2548	1.12×10^{-17}	1.41 ± 0.01	(*63*)
SO_2	1.343(*62*)	1333	1.47×10^{-17}	1.36	(*72*)
H_2O	0.97(*73*)	1650	1.0×10^{-17}	1.26 ± 0.01	(*74, 75*)

Table S9. Physical parameters for Monte Carlo Simulations using CASINO v2.42 software suite.(*66*)

Ice Mixture	Density (g cm^{-3})	99% Penetration Depth (nm)	Dose (eV $molecule^{-1}$)
SO_2	1.343	500 ± 50	19 ± 2
SO_2/H_2O	1.16	540 ± 50	21 ± 2 / 6 ± 1
H_2S/H_2O	0.96	640 ± 60	11 ± 1 / 6 ± 1
SO_2/H_2S	1.14	600 ± 60	18 ± 2 / 10 ± 1

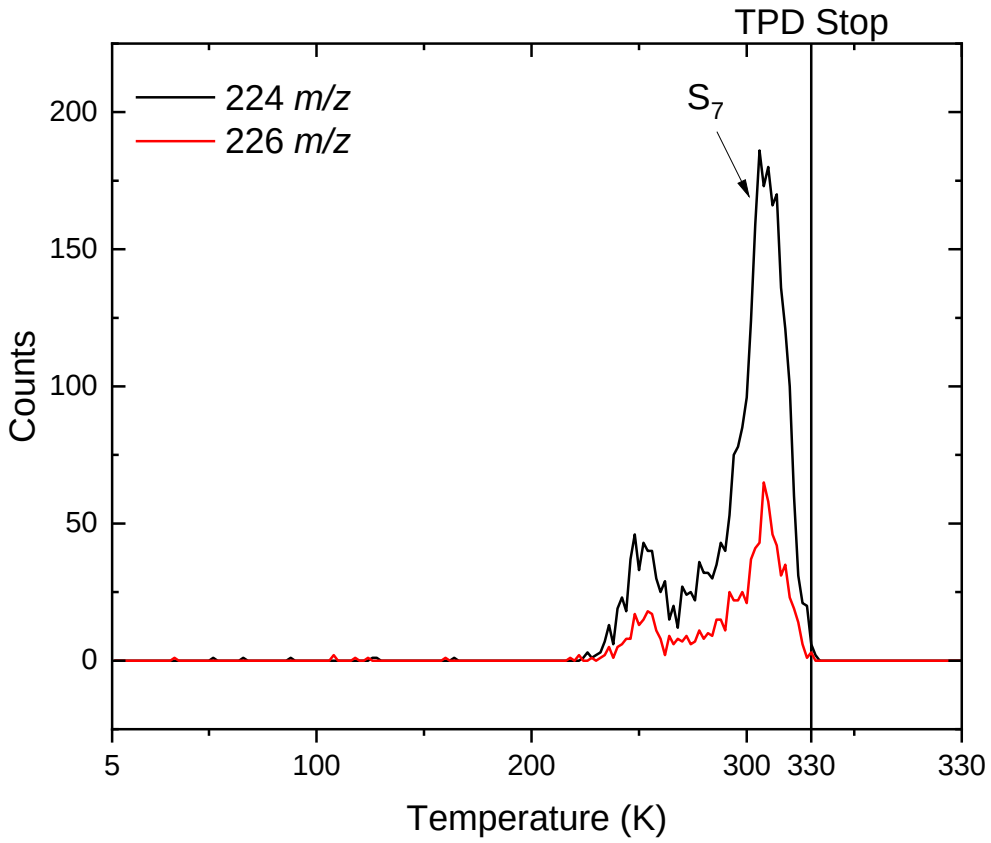

Figure S5. TPD-PI-ReToF-MS of *m/z* = 224 and 226 in the SO_2 ice recorded at 8.75 eV. The mass spectra reveals two sublimation events; one correlating to S_7 which peaks at 312 K.

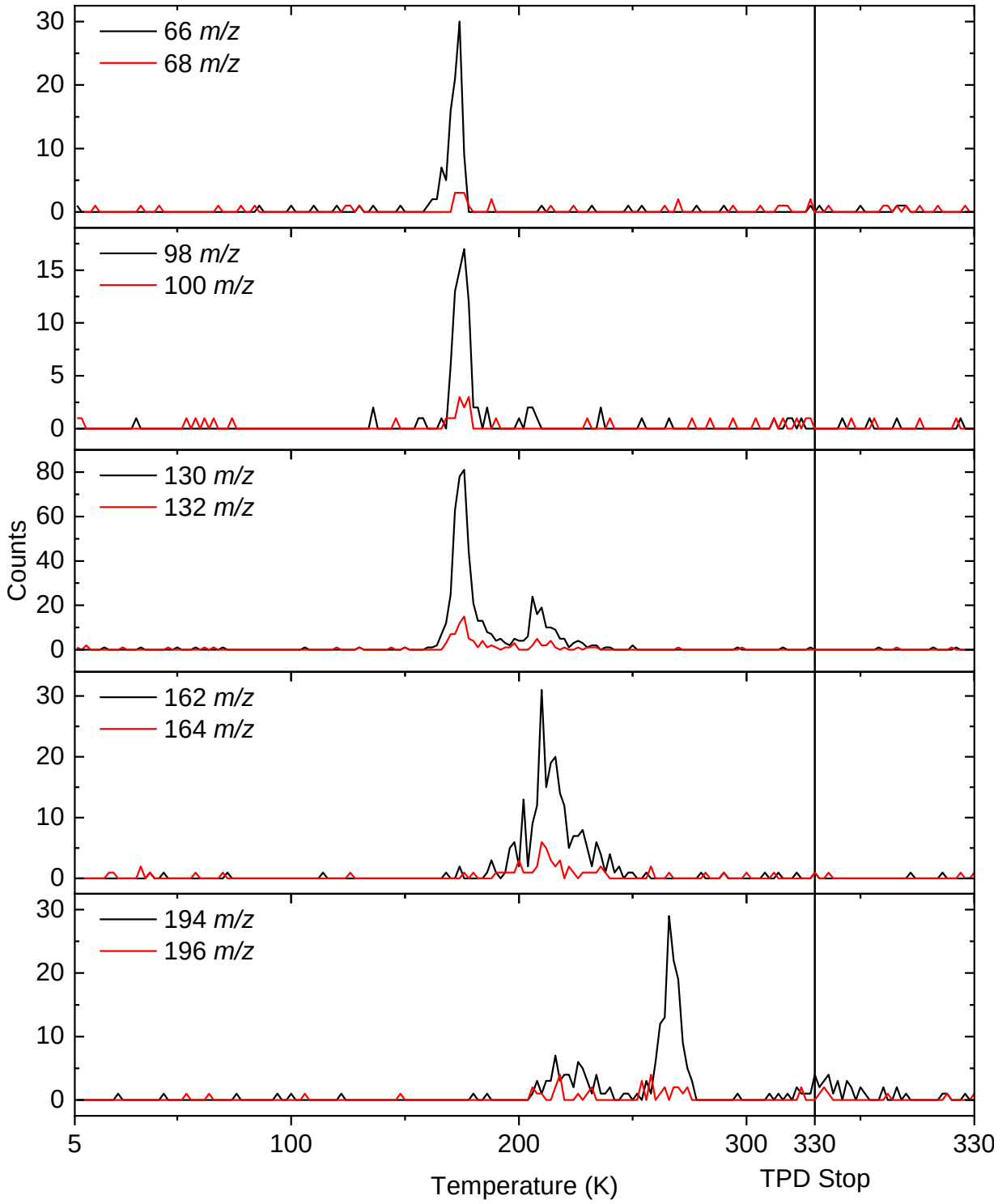

Figure S6. TPD-PI-ReToF-MS recording of mass channels associated with sulfanes (H_2S_n) in the SO_2/H_2O ice experiment with a photon energy of 9.34 eV. These mass channels correlate to H_2S_2 (66 *m/z*), H_2S_3 (98 *m/z*), H_2S_4 (130 *m/z*), H_2S_5 (162 *m/z*), H_2S_6 (194 *m/z*) and their corresponding ^{34}S isotopologues.

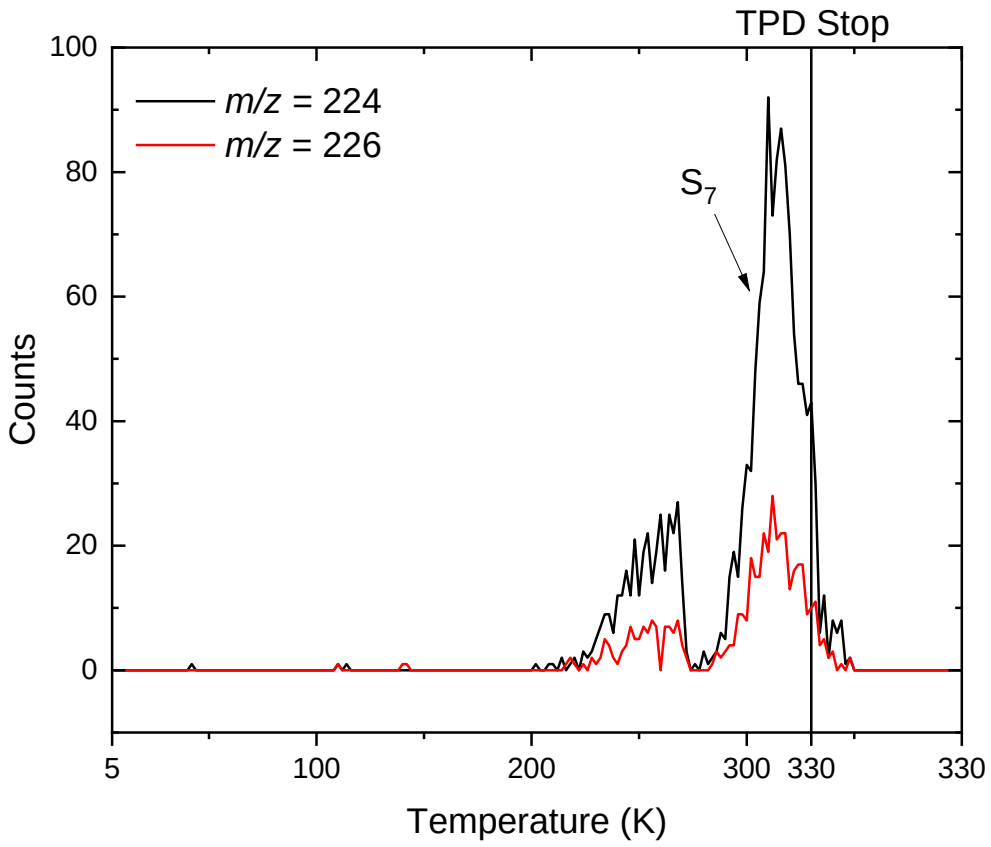

Figure S7. TPD-PI-ReToF-MS of *m/z* = 224 and 226 *m/z* in the SO_2/H_2O ice using 8.75 eV photon energy. The mass spectra reveals two sublimation events; one correlating to S_7 which peaks at 312 K.

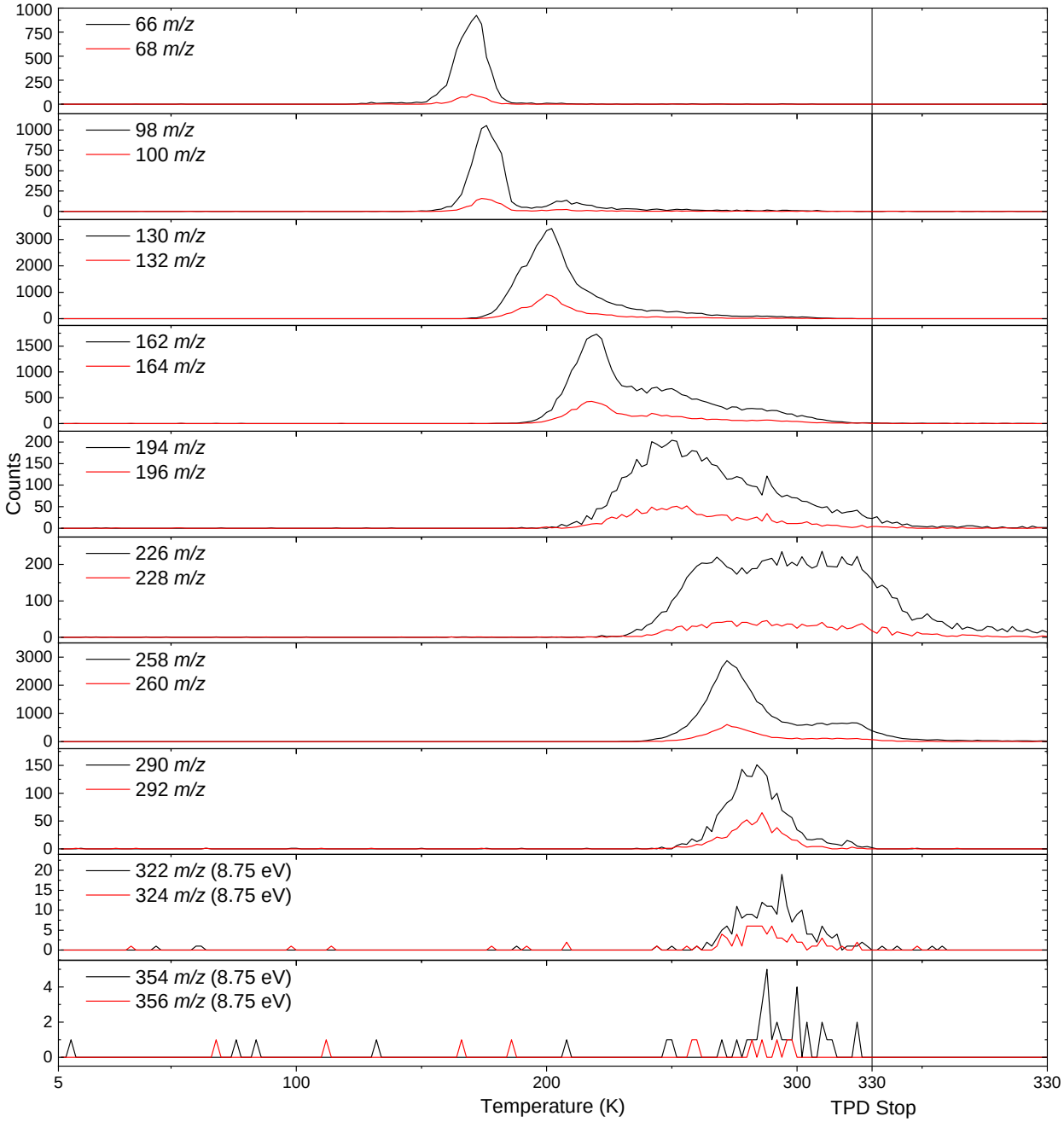

Figure S8. TPD-PI-ToF-MS of the H_2S/H_2O ices at 9.34 and 8.75 eV in mass channels associated with sulfanes (H_2S_n). During TPD, hydrogen disulfide (H_2S_2; 66 *m/z*), H_2S_3 (98 *m/z*), H_2S_4 (130 *m/z*), H_2S_5 (162 *m/z*), H_2S_6 (194 *m/z*), H_2S_7 (226 *m/z*), H_2S_8 (258 *m/z*), H_2S_9 (290 *m/z*), H_2S_{10} (322 *m/z*), H_2S_{11} (354 *m/z*), and their corresponding ^{34}S isotopologues sublime and subsequently detected *via* photoionization reflectron time-of-flight mass spectrometry.

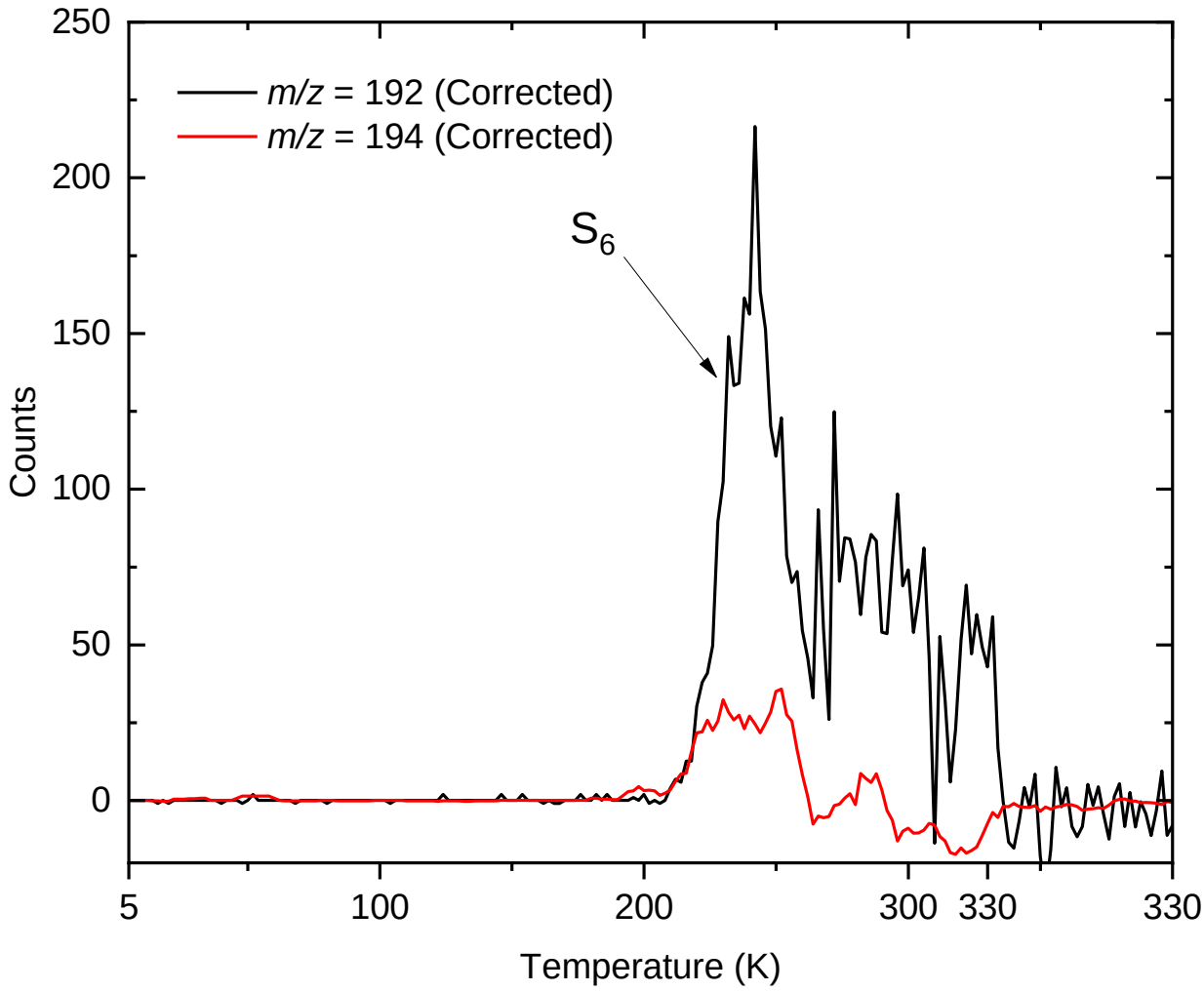

Figure S9. TPD-PI-ToF-MS of the H_2S/H_2O ices at 9.34 eV in mass channels associated with S_6 (192 *m/z*). The spectra at *m/z* = 192 and 194 were corrected for fragmentation of H_2S_7 (*m/z* = 226) by normalizing and subtracting the signal. The corrected spectra must only derive from S_6 which sublimes at 240 K.

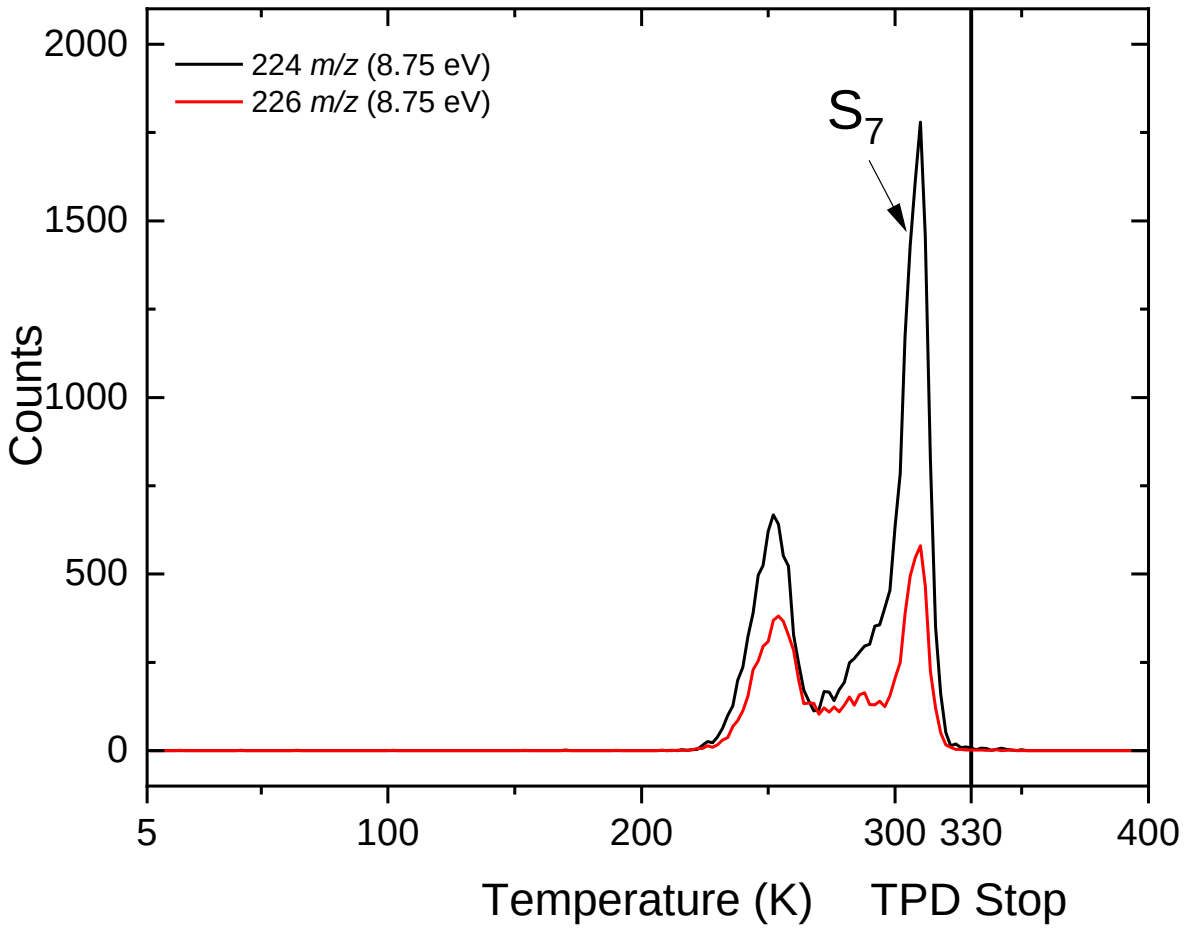

Figure S10. TPD-PI-ToF-MS of the H_2S/H_2O ices at 8.75 eV in mass channels associated with S_7 (224 *m/z*). The mass spectra reveal two sublimation events; one correlating to S_7 which peaks at 306 K.

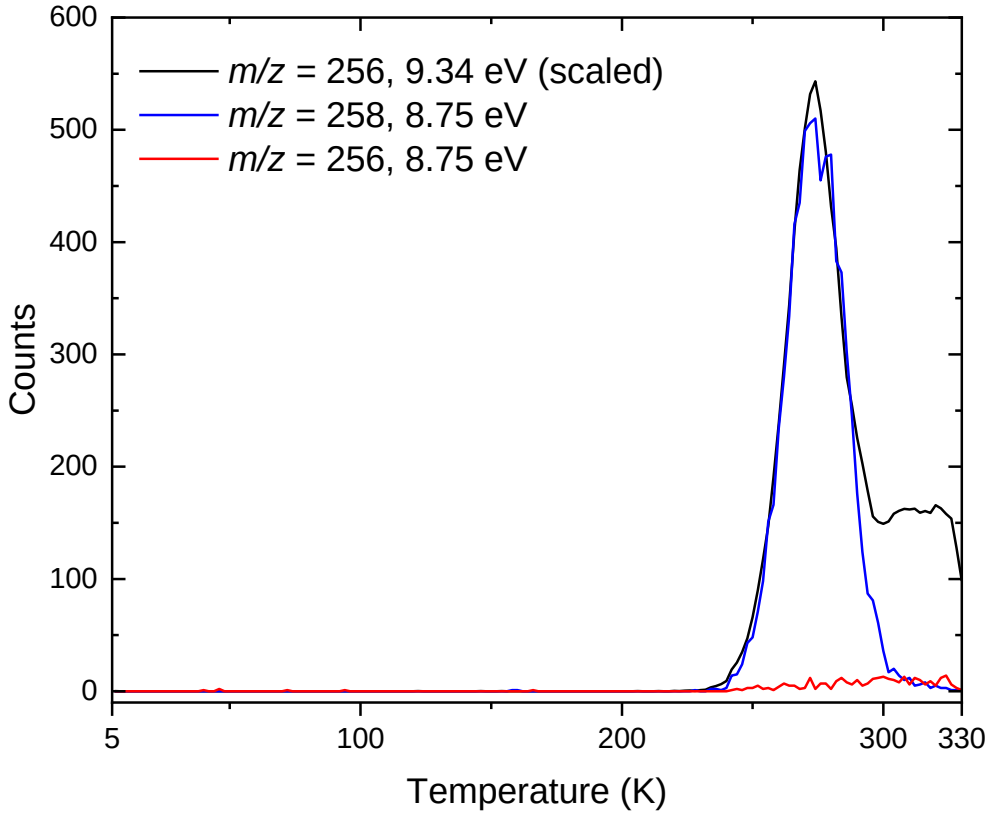

Figure S11. TPD-ReToF-MS of the irradiated H_2S/H_2O ices associated with fragmentation of sulfanes towards allotropes of sulfur. The recorded mass-to-charge of 256 (S_8; black) using 9.34 eV photons, 258 (H_2S_8; blue) using 8.75 eV photons, and 256 (S_8; red) using 8.75 eV photons to compare fragmentation of H_2S_8 to S_8.

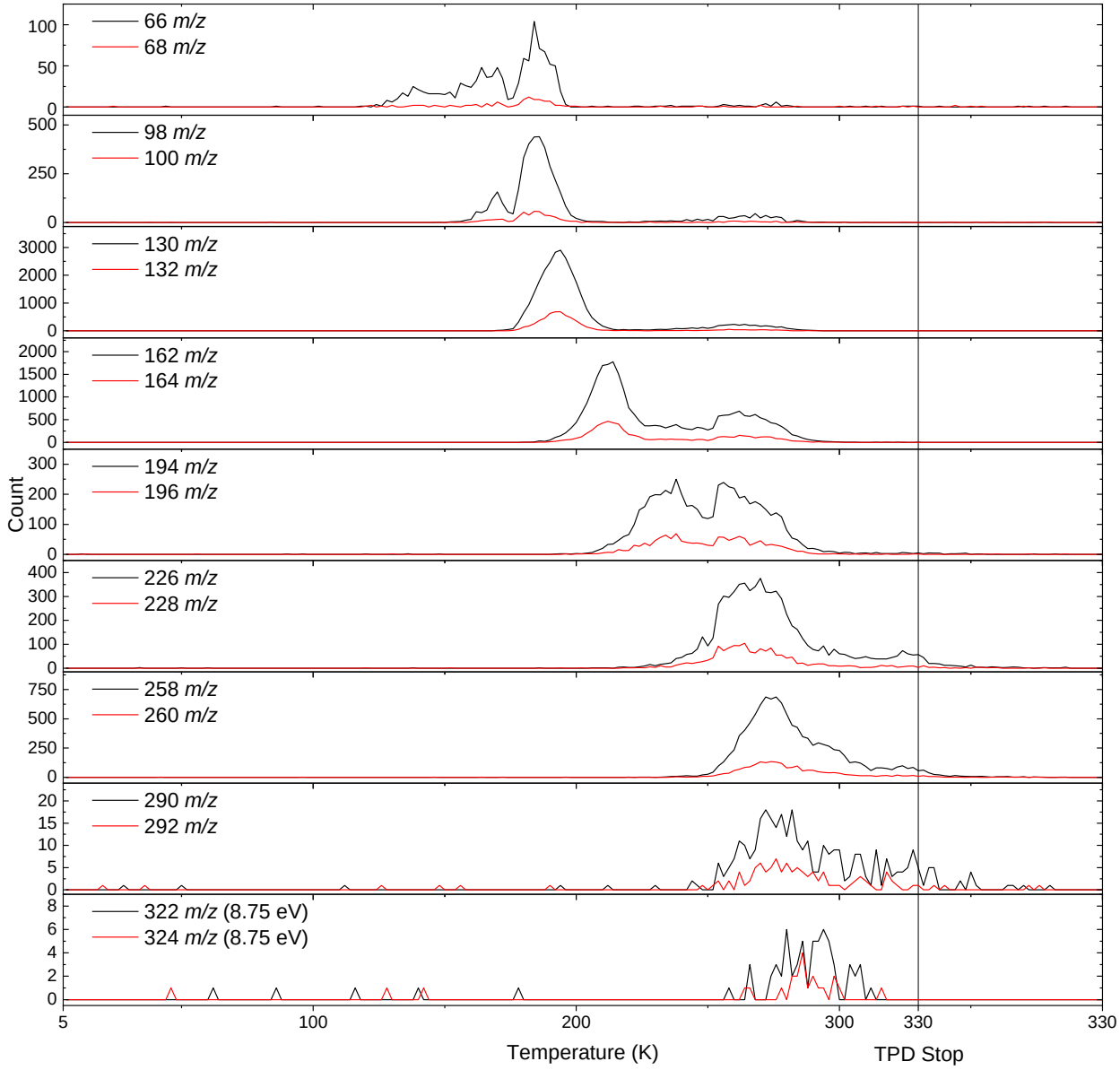

Figure S12. TPD-PI-ToF-MS of the SO_2/H_2S ices at 9.34 and 8.75 eV in mass channels associated with sulfanes. During TPD, hydrogen disulfide (H_2S_2; 66 *m/z*), H_2S_3 (98 *m/z*), H_2S_4 (130 *m/z*), H_2S_5 (162 *m/z*), H_2S_6 (194 *m/z*), H_2S_7 (226 *m/z*), H_2S_8 (258 *m/z*), H_2S_9 (290 *m/z*), H_2S_{10} (322 *m/z*) and their corresponding ^{34}S isotopologues sublime and subsequently detected *via* photoionization reflectron time-of-flight mass spectrometry.

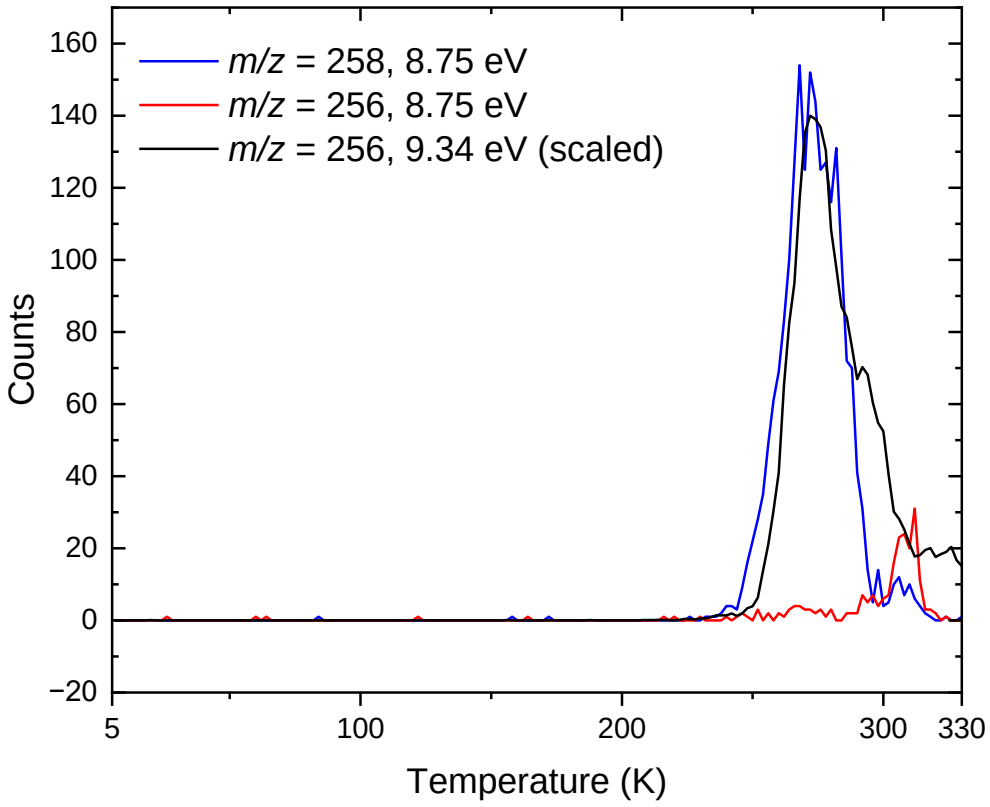

Figure S13. TPD-ReToF-MS of the irradiated SO_2/H_2S ices associated with fragmentation of sulfanes towards allotropes of sulfur. The recorded mass-to-charge of 256 (S_8; black) using 9.34 eV photons, 258 (H_2S_8; blue) using 8.75 eV photons, and 256 (S_8; red) using 8.75 eV photons to compare fragmentation of H_2S_8 to S_8.

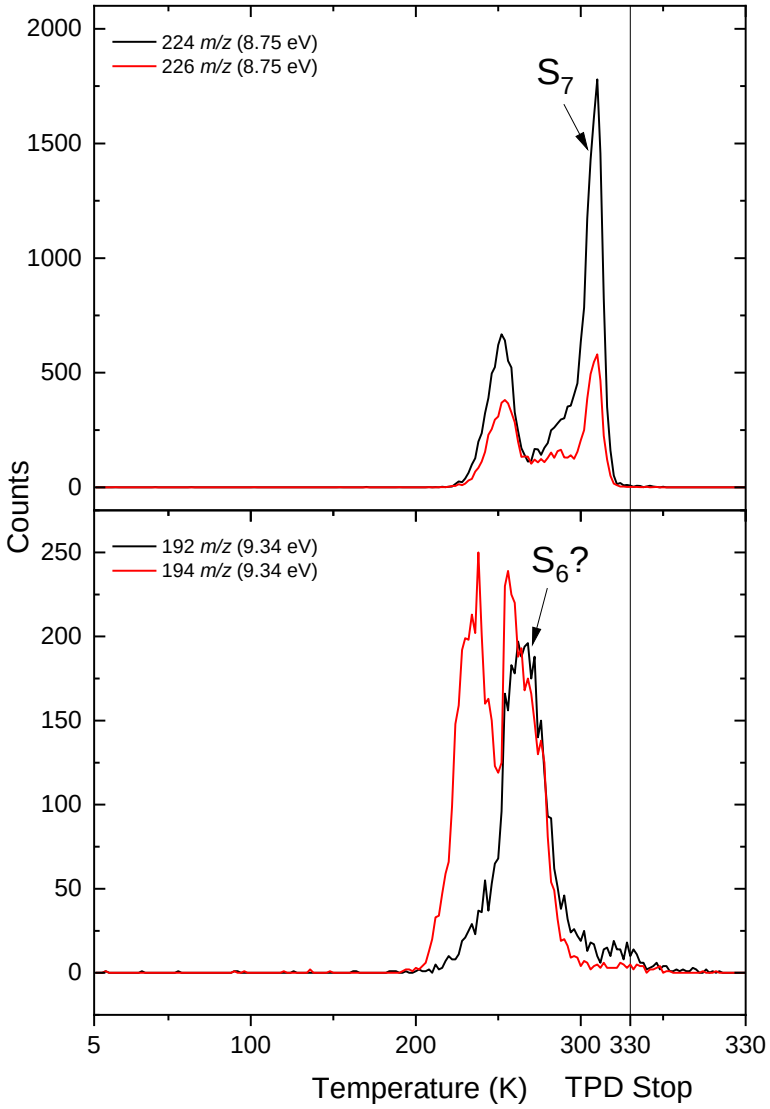

Figure S14. TPD-PI-ToF-MS of the SO_2/H_2S ices at 9.34 and 8.75 eV in mass channels associated with allotropes S_6 and S_7. Allotropes like S_7 (224 *m/z*) and tentatively S_6 (192 *m/z*) can be found subliming during TPD and subsequently ionized and detected *via* reflectron time-of-flight mass spectrometry.

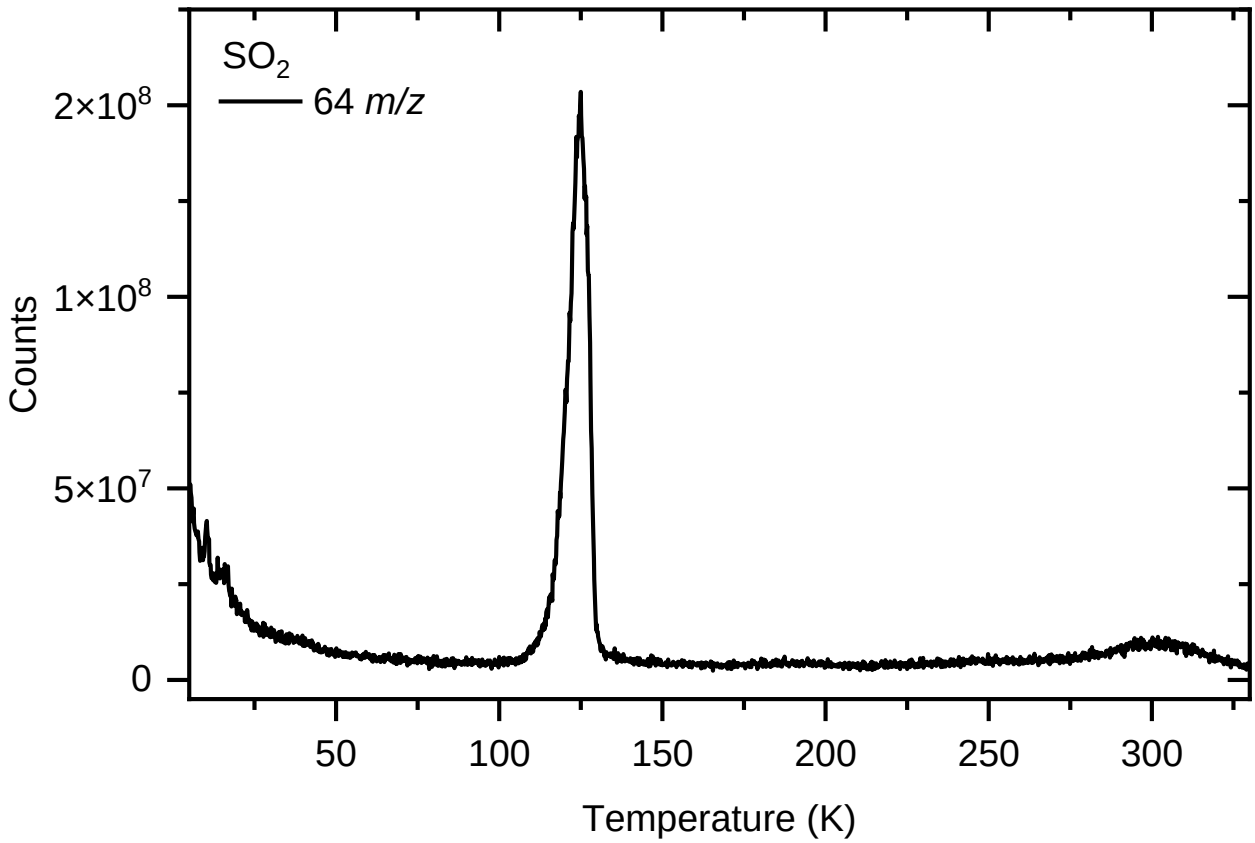

Figure S15. Mass spectra of sulfur dioxide (SO_2) in the pure SO_2 ice experiment. Sulfur dioxide (64 *m/z*) was recorded during TPD from 5-330 K.

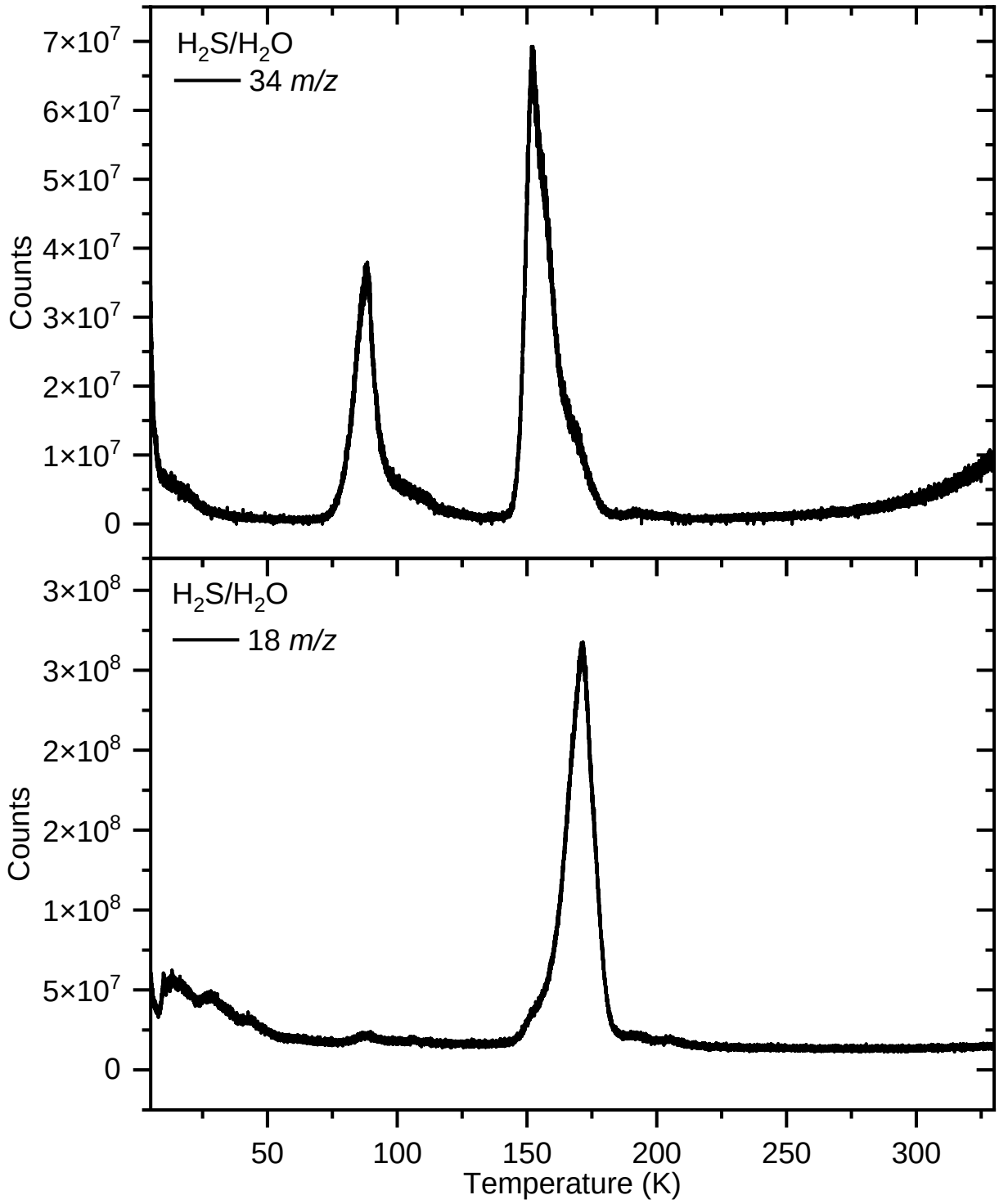

Figure S16. Mass channels of reagents in the hydrogen sulfide (H_2S)/water (H_2O) ice experiment. Hydrogen sulfide (34 *m/z*; top) and water (18 *m/z*; bottom) were recorded during TPD from 5-330 K.

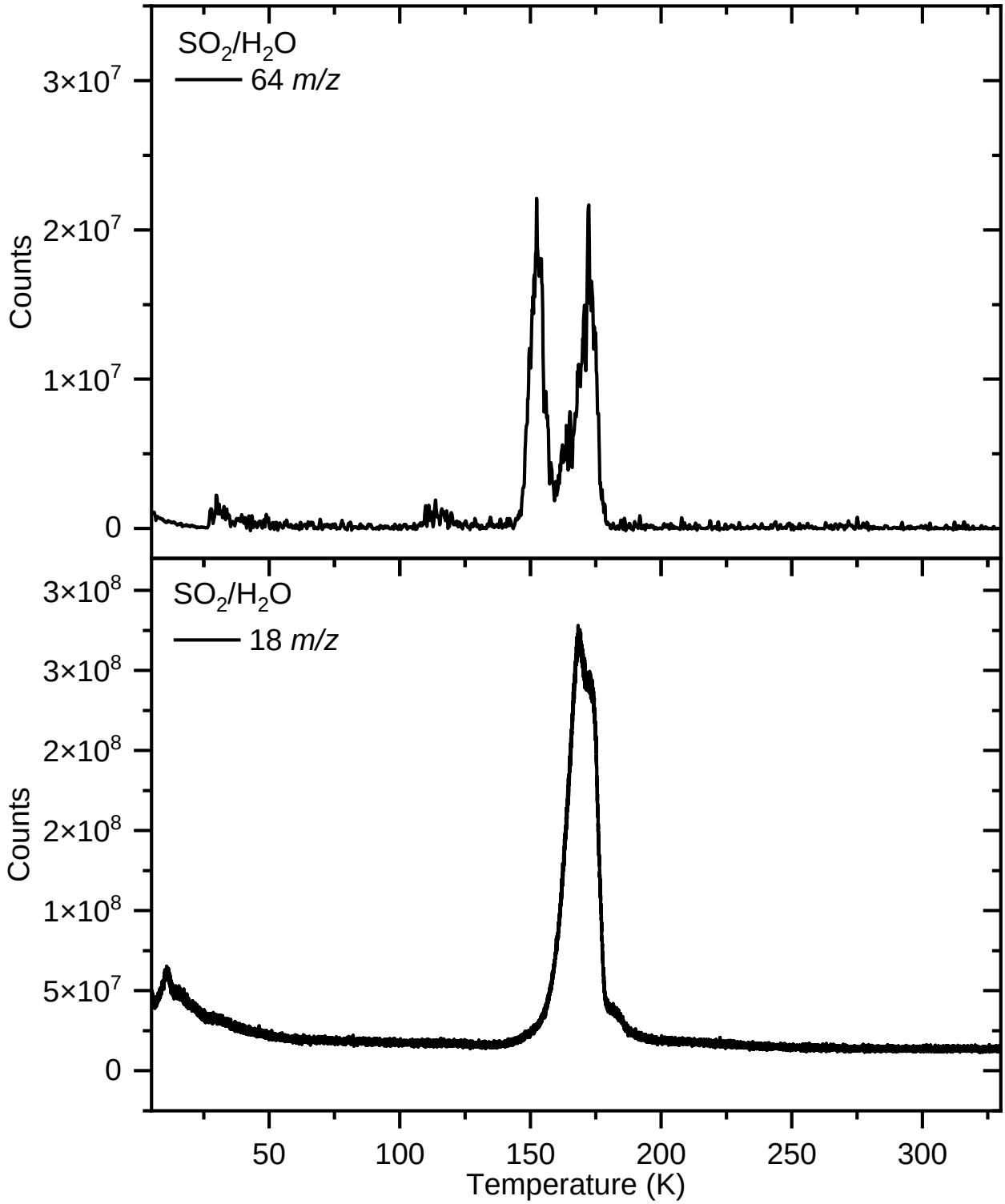

Figure S17. Mass channels of reagents in the sulfur dioxide (SO_2)/water (H_2O) ice experiment. Sulfur dioxide (64 *m/z*; top) and water (18 *m/z*; bottom) were recorded during TPD from 5-330 K.

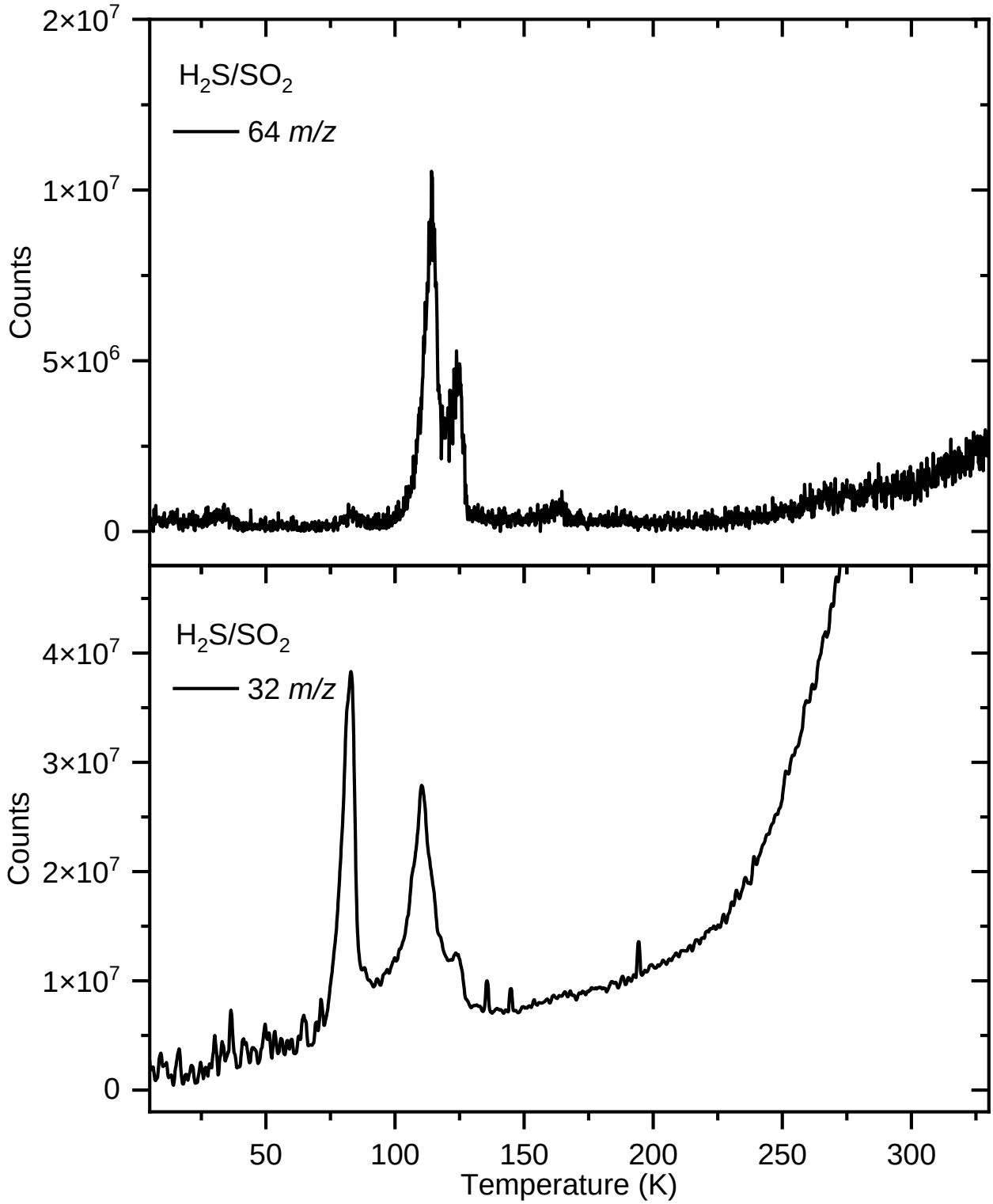

Figure S18. Mass channels of reagents in the hydrogen sulfide (H_2S)/sulfur dioxide (SO_2) ice experiment. Sulfur dioxide (64 *m/z*; top) and hydrogen sulfide (34 *m/z*; bottom) were recorded during TPD from 5-330 K.

REFERENCES

1. T. Yoshimura, Y. Takano, H. Naraoka, T. Koga, D. Araoka, N. O. Ogawa, P. Schmitt-Kopplin, N. Hertkorn, Y. Oba, J. P. Dworkin, J. C. Aponte, T. Yoshikawa, S. Tanaka, N. Ohkouchi, M. Hashiguchi, H. McLain, E. T. Parker, S. Sakai, M. Yamaguchi, T. Suzuki, T. Yokoyama, H. Yurimoto, T. Nakamura, T. Noguchi, Hayabusa2-initial-analysis SOM team, Chemical evolution of primordial salts and organic sulfur molecules in the asteroid 162173 Ryugu. *Nat. Commun.* **14**, 5284 (2023).

2. A. N. Nguyen, P. Mane, L. P. Keller, L. Piani, Y. Abe, J. Aléon, C. M. O. D. Alexander, S. Amari, Y. Amelin, K.-i. Bajo, M. Bizzarro, A. Bouvier, R. W. Carlson, M. Chaussidon, B.-G. Choi, N. Dauphas, A. M. Davis, T. Di Rocco, W. Fujiya, R. Fukai, I. Gautam, M. K. Haba, Y. Hibiya, H. Hidaka, H. Homma, P. Hoppe, G. R. Huss, K. Ichida, T. Iizuka, T. R. Ireland, A. Ishikawa, S. Itoh, N. Kawasaki, N. T. Kita, K. Kitajima, T. Kleine, S. Komatani, A. N. Krot, M.-C. Liu, Y. Masuda, K. D. McKeegan, M. Morita, K. Motomura, F. Moynier, I. Nakai, K. Nagashima, D. Nesvorný, L. Nittler, M. Onose, A. Pack, C. Park, L. Qin, S. S. Russell, N. Sakamoto, M. Schönbächler, L. Tafla, H. Tang, K. Terada, Y. Terada, T. Usui, S. Wada, M. Wadhwa, R. J. Walker, K. Yamashita, Q.-Z. Yin, T. Yokoyama, S. Yoneda, E. D. Young, H. Yui, A.-C. Zhang, T. Nakamura, H. Naraoka, T. Noguchi, R. Okazaki, K. Sakamoto, H. Yabuta, M. Abe, A. Miyazaki, A. Nakato, M. Nishimura, T. Okada, T. Yada, K. Yogata, S. Nakazawa, T. Saiki, S. Tanaka, F. Terui, Y. Tsuda, S.-i. Watanabe, M. Yoshikawa, S. Tachibana, H. Yurimoto, Abundant presolar grains and primordial organics preserved in carbon-rich exogenous clasts in asteroid Ryugu. *Sci. Adv.* **9**, eadh1003 (2023).

3. M. J. Mumma, S. B. Charnley, The chemical composition of comets—Emerging taxonomies and natal heritage. *Annu. Rev. Astron. Astrophys.* **49**, 471–524 (2011).

4. J. R. Cronin, S. Chang, "Organic matter in meteorites: Molecular and isotopic analyses of the murchison meteorite," in *The Chemistry of Life's Origins*, J. M. Greenberg, C. X. Mendoza-Gómez, V. Pirronello, Eds. (Springer Netherlands, 1993), pp. 209–258.

5. M. Tang, S.-L. Qin, T. Liu, L. A. Zapata, X. Liu, Y. Peng, F. Xu, C. Zhang, K. I. Tatematsu, A survey of sulfur-bearing molecular lines toward the dense cores in 11 massive protoclusters. *Astrophys. J. Suppl. Ser.* **275**, 25 (2024).

6. D. V. Mifsud, P. Herczku, R. Ramachandran, P. Sundararajan, K. K. Rahul, S. T. S. Kovács, B. Sulik, Z. Juhász, R. Rácz, S. Biri, Z. Kaňuchová, S. Ioppolo, B. Sivaraman, R. W. McCullough, N. J. Mason, A systematic mid-infrared spectroscopic study of thermally processed H_2S ices. *Spectrochim. Acta A* **319**, 124567 (2024).

7. J. Zhou, Y. Zhao, C. S. Hansen, J. Yang, Y. Chang, Y. Yu, G. Cheng, Z. Chen, Z. He, S. Yu, H. Ding, W. Zhang, G. Wu, D. Dai, C. M. Western, M. N. R. Ashfold, K. Yuan, X. Yang, Ultraviolet photolysis of H_2S and its implications for SH radical production in the interstellar medium. *Nat. Commun.* **11**, 1547 (2020).

8. J. C. Santos, H. Linnartz, K.-J. Chuang, Interaction of H_2S with H atoms on grain surfaces under molecular cloud conditions. *Astron. Astrophys.* **678**, A112 (2023).

9. A. Penzias, P. Solomon, R. Wilson, K. Jefferts, Interstellar carbon monosulfide. *Astrophys. J.* **168**, L53 (1971).

10. M. Oppenheimer, A. Dalgarno, The chemistry of sulfur in interstellar clouds. *Astrophys. J.* **187**, 231–236 (1974).

11. P. M. Gondhalekar, Depletion of sulphur in the interstellar medium. *Mon. Not. R. Astron. Soc.* **217**, 585–588 (1985).

12. D. P. Ruffle, T. W. Hartquist, P. Caselli, D. A. Williams, The sulphur depletion problem. *Mon. Not. R. Astron. Soc.* **306**, 691–695 (1999).

13. M. Kama, O. Shorttle, A. S. Jermyn, C. P. Folsom, K. Furuya, E. A. Bergin, C. Walsh, L. Keller, Abundant refractory sulfur in protoplanetary disks. *Astrophys. J.* **885**, 114 (2019).

14. D. J. Hollenbach, H. A. Thronson Jr., *Interstellar Processes: Proceedings of the Symposium on Interstellar Processes, Held in Grand Teton National Park, July 1986* (Springer Science & Business Media, 2012), vol. 134.

15. E. B. Jenkins, A unified representation of gas-phase element depletions in the interstellar medium. *Astrophys. J.* **700**, 1299–1348 (2009).

16. A. Tieftrunk, G. Pineau des Forets, P. Schilke, C. M. Walmsley, SO and H_2S in low density molecular clouds. *Astron. Astrophys.* **289**, 579–596 (1994).

17. C. M. Walmsley, D. Flower, Complete depletion in prestellar cores. *Astron. Astrophys.* **418**, 1035–1043 (2004).

18. R. Friesen, J. Di Francesco, T. Bourke, P. Caselli, J. Jørgensen, J. Pineda, M. Wong, Revealing H_2D^+ depletion and compact structure in starless and protostellar cores with ALMA. *Astrophys. J.* **797**, 27 (2014).

19. L. Mattsson, Modelling dust processing and the evolution of grain sizes in the ISM using the method of moments. *Planet. Space Sci.* **133**, 107–123 (2016).

20. M. K. McClure, W. R. M. Rocha, K. M. Pontoppidan, N. Crouzet, L. E. U. Chu, E. Dartois, T. Lamberts, J. A. Noble, Y. J. Pendleton, G. Perotti, D. Qasim, M. G. Rachid, Z. L. Smith, F. Sun, T. L. Beck, A. C. A. Boogert, W. A. Brown, P. Caselli, S. B. Charnley, H. M. Cuppen, H. Dickinson, M. N. Drozdovskaya, E. Egami, J. Erkal, H. Fraser, R. T. Garrod, D. Harsono, S. Ioppolo, I. Jiménez-Serra, M. Jin, J. K. Jørgensen, L. E. Kristensen, D. C. Lis, M. R. S. McCoustra, B. A. McGuire, G. J. Melnick, K. I. Öberg, M. E. Palumbo, T. Shimonishi, J. A. Sturm, E. F. van Dishoeck, H. Linnartz, An Ice Age JWST inventory of dense molecular cloud ices. *Nat. Astron.* **7**, 431–443 (2023).

21. A. A. Boogert, P. A. Gerakines, D. C. Whittet, Observations of the icy universe. *Annu. Rev. Astron. Astrophys.* **53**, 541–581 (2015).

22. A. Boogert, W. Schutte, F. Helmich, A. Tielens, D. Wooden, Infrared observations and laboratory simulations of interstellar CH_4 and SO_2. *Astron. Astrophys.* **317**, 929–941 (1997).

23. P. M. Woods, A. Occhiogrosso, S. Viti, Z. Kaňuchová, M. E. Palumbo, S. D. Price, A new study of an old sink of sulphur in hot molecular cores: The sulphur residue. *Mon. Not. R. Astron. Soc.* **450**, 1256–1267 (2015).

24. D. P. Glavin, J. P. Dworkin, C. M. O. D. Alexander, J. C. Aponte, A. A. Baczynski, J. J. Barnes, H. A. Bechtel, E. L. Berger, A. S. Burton, P. Caselli, A. H. Chung, S. J. Clemett, G.

D. Cody, G. Dominguez, J. E. Elsila, K. K. Farnsworth, D. I. Foustoukos, K. H. Freeman, Y. Furukawa, Z. Gainsforth, H. V. Graham, T. Grassi, B. M. Giuliano, V. E. Hamilton, P. Haenecour, P. R. Heck, A. E. Hofmann, C. H. House, Y. Huang, H. H. Kaplan, L. P. Keller, B. Kim, T. Koga, M. Liss, H. L. McLain, M. A. Marcus, M. Matney, T. J. McCoy, O. M. McIntosh, A. Mojarro, H. Naraoka, A. N. Nguyen, M. Nuevo, J. A. Nuth, Y. Oba, E. T. Parker, T. S. Peretyazhko, S. A. Sandford, E. Santos, P. Schmitt-Kopplin, F. Seguin, D. N. Simkus, A. Shahid, Y. Takano, K. L. Thomas-Keprta, H. Tripathi, G. Weiss, Y. Zheng, N. G. Lunning, K. Righter, H. C. Connolly, D. S. Lauretta, Abundant ammonia and nitrogen-rich soluble organic matter in samples from asteroid (101955) Bennu. *Nat. Astron.* **9**, 199–210 (2025).

25. C. Druard, V. Wakelam, Polysulphanes on interstellar grains as a possible reservoir of interstellar sulphur. *Mon. Not. R. Astron. Soc.* **426**, 354–359 (2012).

26. D. V. Mifsud, P. Herczku, R. Rácz, K. K. Rahul, S. T. S. Kovács, Z. Juhász, B. Sulik, S. Biri, R. W. McCullough, Z. Kaňuchová, S. Ioppolo, P. A. Hailey, N. J. Mason, Energetic electron irradiations of amorphous and crystalline sulphur-bearing astrochemical ices. *Front. Chem.* **10**, 1003163 (2022).

27. C. N. Shingledecker, T. Lamberts, J. C. Laas, A. Vasyunin, E. Herbst, J. Kästner, P. Caselli, Efficient production of S_8 in interstellar ices: The effects of cosmic-ray-driven radiation chemistry and nondiffusive bulk reactions. *Astrophys. J.* **888**, 52 (2020).

28. M. Garozzo, D. Fulvio, Z. Kanuchova, M. E. Palumbo, G. Strazzulla, The fate of S-bearing species after ion irradiation of interstellar icy grain mantles. *Astron. Astrophys.* **509**, A67 (2010).

29. J. C. Santos, J. Enrique-Romero, T. Lamberts, H. Linnartz, K.-J. Chuang, Formation of S-bearing complex organic molecules in interstellar clouds via ice reactions with C_2H_2, HS, and Atomic H. *ACS Earth Space Chem.* **8**, 1646–1660 (2024).

30. M. McAnally, J. Bocková, A. Herath, A. M. Turner, C. Meinert, R. I. Kaiser, Abiotic formation of alkylsulfonic acids in interstellar analog ices and implications for their detection on Ryugu. *Nat. Commun.* **15**, 4409 (2024).

31. B. Meyer, Solid allotropes of sulfur. *Chem. Rev.* **64**, 429–451 (1964).

32. P. Ferrari, G. Berden, B. Redlich, L. B. F. M. Waters, J. M. Bakker, Laboratory infrared spectra and fragmentation chemistry of sulfur allotropes. *Nat. Commun.* **15**, 5928 (2024).

33. W. Hagen, A. Tielens, J. Greenberg, The infrared spectra of amorphous solid water and ice I_c between 10 and 140 K. *Chem. Phys.* **56**, 367–379 (1981).

34. K. Fathe, J. S. Holt, S. P. Oxley, C. J. Pursell, Infrared spectroscopy of solid hydrogen sulfide and deuterium sulfide. *J. Phys. Chem. A* **110**, 10793–10798 (2006).

35. S. Maity, R. I. Kaiser, Electron irradiation of carbon disulfide-oxygen ices: Toward the formation of sulfur-bearing molecules in interstellar ices. *Astrophys. J.* **773**, 184 (2013).

36. H. Wieser, P. Krueger, E. Muller, J. Hyne, Vibrational spectra and a force field for H_2S_3 and H_2S_4. *Can. J. Chem.* **47**, 1633–1637 (2011).

37. N. Zengin, P. A. Giguère, Infrared spectrum of crystalline H_2S_2. *Can. J. Chem.* **37**, 632–634 (1959).

38. G. Socrates, *Infrared and Raman Characteristic Group Frequencies* (Wiley, ed. 3, 2004).

39. A. M. Turner, R. I. Kaiser, Exploiting photoionization reflectron time-of-flight mass spectrometry to explore molecular mass growth processes to complex organic molecules in interstellar and solar system ice analogs. *Acc. Chem. Res.* **53**, 2791–2805 (2020).

40. M. J. Abplanalp, M. Förstel, R. I. Kaiser, Exploiting single photon vacuum ultraviolet photoionization to unravel the synthesis of complex organic molecules in interstellar ices. *Chem. Phys. Lett.* **644**, 79–98 (2016).

41. A. Herath, M. McAnally, A. M. Turner, J. Wang, J. H. Marks, R. C. Fortenberry, J. C. Garcia-Alvarez, S. Gozem, R. I. Kaiser, Missing interstellar sulfur in inventories of polysulfanes and molecular octasulfur crowns. *Nat. Commun.* **16**, 5571 (2025).

42. H.-J. Werner, P. J. Knowles, P. Celani, W. Györffy, A. Hesselmann, D. Kats, G. Knizia, A. Köhn, T. Korona, D. Kreplin, R. Lindh, Q. Ma, F. R. Manby, A. Mitrushenkov, G. Rauhut, M. Schütz, K. R. Shamasundar, T. B. Adler, R. D. Amos, S. J. Bennie, A. Bernhardsson, A. Berning, J. A. Black, P. J. Bygrave, R. Cimiraglia, D. L. Cooper, D. Coughtrie, M. J. O. Deegan, A. J. Dobbyn, K. Doll, M. Dornbach, F. Eckert, S. Erfort, E. Goll, C. Hampel, G. Hetzer, J. G. Hill, M. Hodges, T. Hrenar, G. Jansen, C. Köppl, C. Kollmar, S. J. R. Lee, Y. Liu, A. W. Lloyd, R. A. Mata, A. J. May, B. Mussard, S. J. McNicholas, W. Meyer, T. F. Miller, M. E. Mura, A. Nicklass, D. P. O'Neill, P. Palmieri, D. Peng, K. A. Peterson, K. Pflüger, R. Pitzer, I. Polyak, M. Reiher, J. O. Richardson, J. B. Robinson, B. Schröder, M. Schwilk, T. Shiozaki, M. Sibaev, H. Stoll, A. J. Stone, R. Tarroni, T. Thorsteinsson, J. Toulouse, M. Wang, M. Welborn, B. Ziegler, MOLPRO 2023.1, A package of ab initio programs.

43. H.-J. Werner, P. J. Knowles, G. Knizia, F. R. Manby, M. Schütz, Molpro: A general-purpose quantum chemistry program package. *Wiley Interdiscip. Rev. Comput. Mol. Sci.* **2**, 242–253 (2012).

44. M. J. Frisch, G. W. Trucks, H. B. Schlegel, G. E. Scuseria, M. A. Robb, J. R. Cheeseman, G. Scalmani, V. Barone, G. A. Petersson, H. Nakatsuji, X. Li, M. Caricato, A. V. Marenich, J. Bloino, B. G. Janesko, R. Gomperts, B. Mennucci, H. P. Hratchian, J. V. Ortiz, A. F. Izmaylov, J. L. Sonnenberg, D. Williams-Young, F. Ding, F. Lipparini, F. Egidi, J. Goings, B. Peng, A. Petrone, T. Henderson, D. Ranasinghe, V. G. Zakrzewski, J. Gao, N. Rega, G. Zheng, W. Liang, M. Hada, M. Ehara, K. Toyota, R. Fukuda, J. Hasegawa, M. Ishida, T. Nakajima, Y. Honda, O. Kitao, H. Nakai, T. Vreven, K. Throssell, J. A. Montgomery Jr., J. E. Peralta, F. Ogliaro, M. J. Bearpark, J. J. Heyd, E. N. Brothers, K. N. Kudin, V. N. Staroverov, T. A. Keith, R. Kobayashi, J. Normand, K. Raghavachari, A. P. Rendell, J. C. Burant, S. S. Iyengar, J. Tomasi, M. Cossi, J. M. Millam, M. Klene, C. Adamo, R. Cammi, J. W. Ochterski, R. L. Martin, K. Morokuma, O. Farkas, J. B. Foresman, D. J. Fox, Gaussian 16 Revision C.01(Gaussian Inc., 2016).

45. J. Wang, A. M. Turner, J. H. Marks, R. C. Fortenberry, R. I. Kaiser, Formation of Paraldehyde ($C_6H_{12}O_3$) in interstellar analog ices of acetaldehyde exposed to ionizing radiation. *ChemPhysChem* **25**, e202400837 (2024).

46. J. Wang, A. M. Turner, J. H. Marks, C. Zhang, N. F. Kleimeier, A. Bergantini, S. K. Singh, R. C. Fortenberry, R. I. Kaiser, Preparation of acetylenediol (HOCCOH) and glyoxal (HCOCHO) in interstellar analog ices of carbon monoxide and water. *Astrophys. J.* **967**, 79 (2024).

47. J. Wang, J. H. Marks, R. C. Fortenberry, R. I. Kaiser, Interstellar formation of glyceric acid [$HOCH_2CH(OH)COOH$]—The simplest sugar acid. *Sci. Adv.* **10**, eadl3236 (2024).

48. G. Wagner, H. Bock, Photoelektronenspektren und Moleküleigenschaften, XXVI. Die Delokalisation von Schwefel-Elektronenpaaren in Alkylsulfiden und -disulfiden. *Ber. Dtsch. Chem. Ges.* **107**, 68–77 (1974).

49. Z. Kaňuchová, P. Boduch, A. Domaracka, M. E. Palumbo, H. Rothard, G. Strazzulla, Thermal and energetic processing of astrophysical ice analogues rich in SO_2. *Astron. Astrophys.* **604**, A68 (2017).

50. M. H. Moore, R. L. Hudson, R. W. Carlson, The radiolysis of SO_2 and H_2S in water ice: Implications for the icy jovian satellites. *Icarus* **189**, 409–423 (2007).

51. W. Zheng, D. Jewitt, R. I. Kaiser, Formation of hydrogen, oxygen, and hydrogen peroxide in electron-irradiated crystalline water ice. *Astrophys. J.* **639**, 534–548 (2006).

52. R. J. Morton, R. I. Kaiser, Kinetics of suprathermal hydrogen atom reactions with saturated hydrides in planetary and satellite atmospheres. *Planet. Space Sci.* **51**, 365–373 (2003).

53. R. I. Kaiser, K. Roessler, Theoretical and laboratory studies on the interaction of cosmic-ray particles with interstellar ices. III. suprathermal chemistry-induced formation of hydrocarbon molecules in solid methane (CH_4), ethylene (C_2H_4), and acetylene (C_2H_2). *Astrophys. J.* **503**, 959 (1998).

54. B. Ruscic, D. H. Bross, Active Thermochemical Tables (ATcT) values based on ver. 1.220 of the Thermochemical Network, Argonne National Laboratory, Lemont, Illinois, USA (2025).

55. J. Hrbek, S. Y. Li, J. A. Rodriguez, D. G. van Campen, H. H. Huang, G. Q. Xu, Synthesis of sulfur films from S_2 gas: Spectroscopic evidence for the formation of S_n species. *Chem. Phys. Lett.* **267**, 65–71 (1997).

56. S. Millefiori, A. Alparone, Ab initio study of the structure and polarizability of sulfur clusters, S_n (n = 2−12). *J. Phys. Chem. A* **105**, 9489–9497 (2001).

57. M. Kumar, J. S. Francisco, Elemental sulfur aerosol-forming mechanism. *Proc. Natl. Acad. Sci. U.S.A.* **114**, 864–869 (2017).

58. M. H. Matus, D. A. Dixon, K. A. Peterson, J. A. W. Harkless, J. S. Francisco, Coupled-cluster study of the electronic structure and energetics of tetrasulfur, S_4. *J. Chem. Phys.* **127**, 174305 (2007).

59. R. Johnson, CCCBDBD Computational Chemistry Comparison and Benchmark Database (2022); http://cccbdb.nist.gov.

60. M. Fedyaeva, S. Lepeshkin, A. R. Oganov, Stability of sulfur molecules and insights into sulfur allotropy. *Phys. Chem. Chem. Phys.* **25**, 9294–9299 (2023).

61. A. M. Turner, M. J. Abplanalp, S. Y. Chen, Y. T. Chen, A. H. H. Chang, R. I. Kaiser, A photoionization mass spectroscopic study on the formation of phosphanes in low temperature phosphine ices. *Phys. Chem. Chem. Phys.* **17**, 27281–27291 (2015).

62. Y. Y. Yarnall, R. L. Hudson, A new method for measuring infrared band strengths in H_2O ices: First results for OCS, H_2S, and SO_2. *Astrophys. J. Lett.* **931**, L4 (2022).

63. R. L. Hudson, P. A. Gerakines, Infrared spectra and interstellar sulfur: New laboratory results for H_2S and four malodorous thiol ices. *Astrophys. J.* **867**, 138 (2018).

64. M. Bouilloud, N. Fray, Y. Bénilan, H. Cottin, M.-C. Gazeau, A. Jolly, Bibliographic review and new measurements of the infrared band strengths of pure molecules at 25 K: H_2O, CO_2, CO, CH_4, NH_3, CH_3OH, HCOOH and H_2CO. *Mon. Not. R. Astron. Soc.* **451**, 2145–2160 (2015).

65. A. G. Yeghikyan, Irradiation of dust in molecular clouds. II. Doses produced by cosmic rays. *Astrophysics* **54**, 87–99 (2011).

66. D. Drouin, A. R. Couture, D. Joly, X. Tastet, V. Aimez, R. Gauvin, CASINO V2.42—A Fast and easy-to-use modeling tool for scanning electron microscopy and microanalysis users. *Scanning* **29**, 92–101 (2007).

67. R. I. Kaiser, Experimental investigation on the formation of carbon-bearing molecules in the interstellar medium via neutral− neutral reactions. *Chem. Rev.* **102**, 1309–1358 (2002).

68. J. Wang, J. H. Marks, A. M. Turner, A. A. Nikolayev, V. Azyazov, A. M. Mebel, R. I. Kaiser, Mechanistical study on the formation of hydroxyacetone (CH_3COCH_2OH), methyl acetate (CH_3COOCH_3), and 3-hydroxypropanal ($HCOCH_2CH_2OH$) along with their enol tautomers (prop-1-ene-1,2-diol ($CH_3C(OH)CHOH$), prop-2-ene-1,2-diol ($CH_2C(OH)CH_2OH$), 1-methoxyethen-1-ol ($CH_3OC(OH)CH_2$) and prop-1-ene-1,3-diol ($HOCH_2CHCHOH$)) in interstellar ice analogs. *Phys. Chem. Chem. Phys.* **25**, 936–953 (2023).

69. A. Bergantini, S. Góbi, M. J. Abplanalp, R. I. Kaiser, A mechanistical study on the formation of dimethyl ether (CH_3OCH_3) and ethanol (CH_3CH_2OH) in methanol-containing ices and implications for the chemistry of star-forming regions. *Astrophys. J.* **852**, 70 (2018).

70. M. H. Moore, Studies of proton-irradiated SO_2 at low temperatures: Implications for lo. *Icarus* **59**, 114–128 (1984).

71. R. F. Ferrante, M. H. Moore, M. M. Spiliotis, R. L. Hudson, Formation of Interstellar OCS: Radiation chemistry and IR spectra of precursor ices. *Astrophys. J.* **684**, 1210–1220 (2008).

72. M. Garozzo, D. Fulvio, O. Gomis, M. E. Palumbo, G. Strazzulla, H-implantation in SO_2 and CO_2 ices. *Planet. Space Sci.* **56**, 1300–1308 (2008).

73. A. Narten, C.-G. Venkatesh, S. Rice, Diffraction pattern and structure of amorphous solid water at 10 and 77 K. *J. Chem. Phys.* **64**, 1106–1121 (1976).

74. D. M. Hudgins, S. A. Sandford, L. J. Allamandola, A. G. G. M. Tielens, Mid- and far-infrared spectroscopy of ices: Optical constants and integrated absorbances. *Astrophys. J. Suppl. Ser.* **86**, 713 (1993).

75. B. A. Seiber, A. M. Smith, B. E. Wood, P. R. Müller, Refractive indices and densities of H_2O and CO_2 films condensed on cryogenic surfaces. *Appl. Optics* **10**, 2086–2089 (1971).